Polar Polymeric Langmuir−Blodgett Films for Optical Applications

Dzung M. Nguyen, Thomas M. Mayer,† Steven F. Hubbard, Kenneth D. Singer, J. Adin Mann, Jr.,* and Jerome B. Lando*

Departments of Macromolecular Science and Physics, Case Western Reserve University, Cleveland, Ohio 44106, and Sandia National Laboratories, Albuquerque, New Mexico 87185

Received August 19, 1996; Revised Manuscript Received June 23, 1997[⊗]

ABSTRACT: A side-chain liquid crystalline copolymer containing ether−nitrobiphenyl groups was investigated as a nonlinear optical material. Ultrathin films have shown second harmonic generation and therefore have a variety of interesting applications. Waveguides composed of multilayers of the copolymer have been fabricated, and propagation losses as low as 2.3 dB/cm in a lowest order TE mode at 800 nm wavelength have been measured. The second harmonic coefficient is $d_{33} = 42.0 \pm 1.7$ pm/V at the 1064 nm fundamental wavelength and is consistent with an oriented gas model. From spectroscopic ellipsometry measurements the film refractive index is 2.24 ± 0.15 and the extinction coefficient ≤ 0.05 in the visible range of wavelengths. The monolayer and multilayer repeat structures were also studied by X-ray reflectivity and diffraction. The optical thickness and the oscillations in the reflectivity were in reasonable accord with a repeat length of about 3.6 nm.

1. Introduction

The Langmuir−Blodgett (LB) technique allows the fabrication of an ultrathin film with controllable thickness.[1] It involves first spreading insoluble molecules on a water subphase to form a Langmuir monolayer followed by deposition onto a suitable substrate. Successive deposition steps lead to the formation of multilayer films, or LB films.

LB films can have many applications such as alignment layers for large flat-panel liquid crystal displays, nonlinear optical devices, and gas-sensing detectors. Further, thin films fabricated by the LB technique are fundamentally of interest for their novel properties. LB films have received considerable attention as nonlinear optical materials, which for second-order nonlinearities, requires the absence of inversion symmetry. Two principle approaches to achieving noncentrosymmetry waveguides in LB films have been investigated. In the first, alternating layer structures have been fabricated, for example by alternating nonlinear optically active layers with more passive layers.[2] Such structures have produced efficient second harmonic generation in waveguided structures.[3−6] Another approach is to generate a polar direction in the film plane by depositing in an oriented herringbone structure. Such films have also efficiently generated second harmonic signals.[7−10] We have been investigating another approach using liquid crystal copolymers that naturally form z-type films and that are highly polar.[11] The material Cop11 is a liquid crystalline copolymer that has side-chain mesogenic groups, composed of approximately a 50/50 mixture of 4-(10-undecen-1-yloxy)-4′-nitrobiphenyl ($CH_2CH(CH_2)_9O(C_6H_4)_2NO_2$) and 4-(10-undecen-1-yloxy)-4′-[(methoxyethoxy)methoxy]biphenyl ($CH_2CH(CH_2)_9O(C_6H_4)_2OCH_2O(CH_2)_2OCH_3$). (Figure 1 shows a variation of this structure that was also used in this work.) This system exhibits second harmonic generation. The ether−nitrobiphenyl moieties have an electron-accepting and an electron-donating group connected to a delocalized π-electron system. The rectification in the polarization response of molecules can arise through asymmetric displacement of charge. An increase in the difference between the electron affinities of the donor and the acceptor groups or the more nearly planar configuration of the overall π-system leads to an increase in nonlinear hyperpolarizability.[12−14] The chemical requirement for these LB films is the incorporation of a moiety that enhances the nonlinear polarizability of the molecules forming the film. The structure requirement for these LB films is a noncentrosymmetric space group.

In the studies reported herein, our primary objective was to fabricate a waveguide film and measure its relevant parameters such as waveguide loss, the nonlinear optical coefficient, and the film's optical constants and thickness. The secondary objective is to synthesize a set of promising nonlinear optical materials by increasing the number density of the ether−nitrobiphenyl groups. The film thickness and optical constants were obtained from spectroscopic ellipsometry. This technique has been used widely to characterize semiconductor surfaces and thin films of diverse types. However, the interpretation of spectroscopic ellipsometry data of LB layers requires a delicate numerical analysis before the refractive index, extinction coefficient, and thickness information can be estimated. In order to examine the electron periodicity perpendicular to the multilayer surface, synchrotron X-ray reflectivity and X-ray diffraction measurements were carried out. The film thickness can also be obtained from the reflectivity spectra. Modeling is required to gain additional information about film roughness. Subsequently, the rotational Maker fringe method was used to determine the second-order nonlinear optical coefficient. Finally, a waveguide was fabricated using LB techniques and tested.

2. Experimental Section

Synthesis of Cop11,4. Materials. Poly(hydromethylsiloxane) (MN230) and platinum divinyltetramethyldixiloxane catalyst in xylene were obtained from Hüls Chemical. The procedures used in the synthesis of the monomers 4-(10-undecen-1-yloxy)-4′-nitrobiphenyl ($CH_2CH(CH_2)_9O(C_6H_4)_2NO_2$), 4-(3-buten-1-yloxy)-4′-nitrobiphenyl ($CH_2CH(CH_2)_2O(C_6H_4)_2NO_2$), and 4-(10-undecen-1-yloxy)-4′-[(methoxyethoxy-meth-

* To whom correspondence should be addressed at Case Western Reserve University.
† Sandia National Laboratories.
⊗ Abstract published in *Advance ACS Abstracts,* September 15, 1997.

S0024-9297(96)01256-9 CCC: $14.00

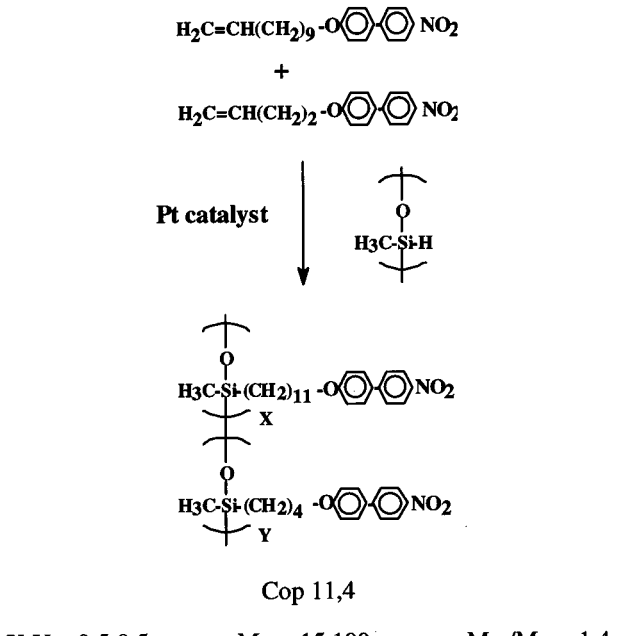

Cop 11,4

X:Y ~ 0.5:0.5 Mn = 15,100 Mw/Mn = 1.4

Earlier Copolymer 11

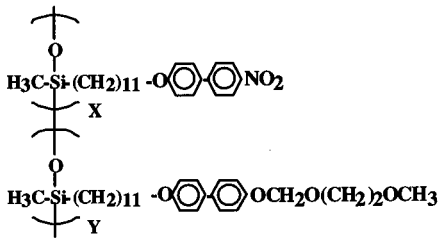

X:Y ~ 0.5:0.5 Mn = 19,200 Mw/Mn = 2.1

Figure 1. Attachment of side chains: 4-(10-undecen-1-yloxy)-4′-nitrobiphenyl and 4-(3-buten-1-yloxy)-4′-nitrobiphenyl to poly(hydromethylsiloxane) in xylene with platinum divinyltetramethyldixiloxane catalyst to obtain the copolymer, Cop11,4. In Cop11 one of the nitrobiphenyl moieties is replaced; see the Introduction for the chemical formula.

oxy]biphenyl ($CH_2CH(CH_2)_9O(C_6H_4)_2OCH_2O(CH_2)_2OCH_3$) were reported previously.[15] All solvents were evaporated using procedures discussed in ref 16.

Characterization. ^{1}H-NMR (200 MHz) spectra were recorded on a Varian XL-200 spectrometer. TMS was used as a standard. The relative molecular weights of the polymers were determined by gel permeation chromatography (GPC) using a Perkin-Elmer series 10 C instrument equipped with a LC-100 column oven and a Nelson Analytical integrator data system. The measurements were made at 40 °C using tetrahydrofuran as a solvent with a UV detector (254 nm). Polystyrene standards were used for the calibration plot.

Hydroxylation. In a flamed-dried 15 mL round bottom flask purged with argon, 0.5221 g (1.42 mmol) of 4-(10-undecen-1-yloxy)-4′-nitrobiphenyl, 0.377 g (1.4 mmol) of 4-(3-buten-1-yloxy)-4′-nitrobiphenyl, 1 mL of tetrahydrofuran, 1.5 mL of toluene, and 0.0513 g of poly(hydromethylsiloxane) were mixed. A rubber stopper, wrapped with Teflon, sealed the flask as the solution temperature was raised to 60 °C. After approximately 50 μL (~0.0551 g) of catalyst was added, the flask was quickly sprayed with argon and sealed tightly with Teflon. The reaction was initially vigorous. A light yellowish solution turned into a clear caramel color. The extent of the reaction was monitored at different times (t = 0, 1, and 2 h) by observing the Si−H stretching band at ~2150 cm^{-1} using a single-beam FTIR instrument (Digi-Lab FTS-60 FTIR). A very small peak could be observed 2 h later. About 2 drops of catalyst was added, and the reaction was run overnight. The reaction mixture was cooled and precipitated in methanol. A rubberlike solid was obtained. It was dissolved in methylene chloride and reprecipitated with ethanol several times to remove the catalyst and residual monomers.

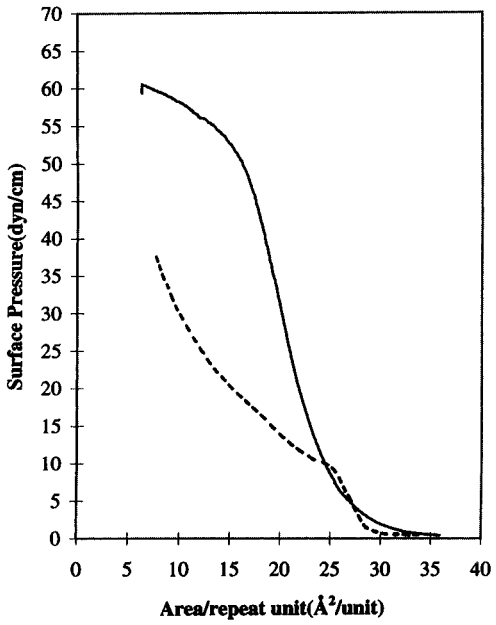

Figure 2. Isotherms (surface−pressure (π) vs area of the repeat unit) for Cop11,4 (dashed) and Cop 11 (solid) at the air−water interface at a temperature of 22 °C.

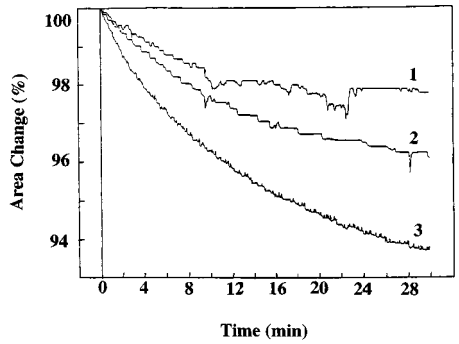

Figure 3. Comparison of compressive creep curves at various surface pressures for Cop 11,4 films. At 5.4 mN/m (1) the film is stable after 30 min. Around the collapsed pressure, 9.5 mN/m (2), the film is unstable, and beyond the surface pressure of 17.4 mN/m (3), the film is unstable as indicated by a continuous decay of the surface pressure with time.

The product from the hydroxylation of 4-(10-undecen-1-yloxy)-4′-nitrobiphenyl and 4-(3-buten-1-yloxy)-4′-nitrobiphenyl is called "Cop11,4" (Figure 1). The results from GPC and ^{1}H-NMR are as follows: GPC M_n = 15 129, M_w/M_n = 1.4; ^{1}H-NMR ($CDCl_3$, δ ppm) a peak was observed at 0.47 ppm (−Si−CH_2−R) but no peaks were observed at 4.7 ppm (−Si−H) and all other positions corresponding to the monomer spectra with the broadening of polymer peaks.[17,18]

Preparation of the LB Film. The surface pressure−area isotherm and creep test data were collected using standard techniques[1,11] to find the best conditions for multilayer formation. The surface pressure−area isotherm (Figure 2) indicates the behavior of the molecule at the air−water interface by monitoring the surface pressure as a function of the average molecular area at a constant temperature. The creep test (Figure 3) indicates surface pressures where the monolayer is stable. Once stability has been established, the monolayer is

then transferred to a suitable substrate. A successful transferring of the monolayer to a substrate is indicated by the deposition ratio ($R = A_{substrate}/A_{subphase}$),[19] where $A_{substrate}$ is the area of the film deposited on the substrate and $A_{subphase}$ is the area of the molecules lost to the substrate. A good deposition has a value of unity.

In the creep test, the film is compressed to a possible operating surface pressure. The monolayer is held at constant pressure, and the area change is recorded.[1,20] The film is taken to be stable when the change in area is less than 3% over a period of 0.5 h.

It has been suggested that the rigidity of the monolayer can be estimated crudely as follows.[21] The film pressure is held constant at a chosen pressure by a control system applied to the moving barrier. Under constant pressure control, a part of the monolayer is removed with a suction tube; the moving barrier should respond quickly and return to the original pressure. A sluggish response suggests that the film has a high surface viscosity. This procedure was used to check the "stiffness" of Cop films. A second measure is that of the elastic modulus computed from the isotherm according to $K_g = -A(\partial\pi/\partial A)_T$.

LB films were prepared on a commercial Lauda trough in a class 10 laminar flow area inside a class 100 clean room. The subphase water was obtained from the treatment of local tap water with an exchange carbon tank, a water softener, and a Millipore water system (Milli-RO 120 and a Milli-Q plus). The resistivity of the water was greater than 18 MΩ cm but still could have been contaminated by surfactant. The "shake-test" was performed to check for surface active contamination of the water; we observed how fast bubbles break after shaking the water in a clean flask. At all times either there was no bubble formation or the few that formed broke in a fraction of a second. The substrates were Corning microscope slides or silicon wafers. The glass slides were stored in concentrated nitric acid for 2 days. They were then ultrasonically agitated for 5 min in methanol, water, and acetone. The silicon wafers were boiled for 30 min in a piranha solution of 30:70 hydrogen peroxide and sulfuric acid. The wafers were rinsed with Millipore water and dried under a stream of pure nitrogen. To obtain a hydrophobic substrate, the clean substrates were exposed to hexamethyldisiloxane (HMDS) vapor for 2 days.

The solvents for Cop11 and Cop11,4 were HPLC grade chloroform and methylene chloride, respectively. The concentration of the solution was 0.2 mg/mL. The initial spreading areas were greater than 100 Å^2/repeat unit. The temperature of the subphase was 22.5 °C. The compression rate for Cop11 was 10.7 (Å^2/repeat unit)/min and for Cop11,4 was (5.8 Å^2/repeat unit)/min. During dipping, the films were maintained at a constant surface pressure: $\pi = 30$ mN/m for Cop11 and $\pi = 5.5$ mN/m for Cop11,4.

The LB layers were built up by X-type horizontal deposition. The substrate was held almost horizontally to the surface with Teflon tweezers, and then allowed to penetrate the monolayer at the air−water interface. Next, the monolayer was suctioned out, and the substrate was withdrawn with its long axis perpendicular to the surface of the water. This deposition process was repeated as many times as necessary to build up the desired film thickness. The deposition ratio of the monolayer was 1:1.1 because the tweezer's handle picked up extra film.

Characterization. Spectroscopic Ellipsometry. The measurements were made with a J. A. Woolam Co. instrument with an automatic, rotating analyzer, and variable angle of incidence. Measurements were carried out to determine the film's refractive index (n), the extinction coefficient (k), and the film thickness (h).[22] The quantities n and k are related to the optical propagation constant by $q = (\omega/c)(n + ik)$. The spectroscopic ellipsometry data were collected at three incident angles, 65, 70, and 75°, at 5 nm intervals over the wavelength range 250−800 nm for the reference−substrate and the film−substrate systems. The raw data were processed using the software provided by the Woolam Co. The model will be described in more detail in the results section. Nine samples of various numbers of monolayers on silicon substrates were analyzed: 1-, 2-, 3-, 4-, and 10-layer films were studied. To check for reproducibility, the samples included three 1-layer, two 2-layer, and two 3-layer LB films. In addition, three silicon substrates were dipped through a water surface without the monolayer at the air−water interface to serve as references.

X-ray Reflectivity and Diffraction. The measurements were done at Brookhaven National Laboratory. The X-ray source was the National Synchrotron Light Source (beam line X-23B, $\lambda = 1.628$ Å). The slit size for the outgoing beam was 2×2 mm^2, and the slit size for the position sensitive detector was 1×1 mm^2. The X-rays were monitored with scintillation detectors. A typical reflection scan took 1−2 h and the intensities of the reflected beam, I, were normalized to the intensity of the incident beam, I_0. The reflectivities of films of 1, 2, 3, and 10 LB layers deposited on silicon substrates were measured.

Second Harmonic Generation. The method used to determine the relative nonlinear coefficient was the rotational Maker fringe method.[23] A pulsed Nd:YAG laser ($\lambda = 1.06$ μm) beam was sent through the film, which was placed on a rotational stage with its axis perpendicular to the beam. The amount of second harmonic light ($\lambda = 532$ nm) was recorded as a function of the incident angle. The second-order nonlinear susceptibility for the Cop11 film was calculated using the rotational Maker fringe analysis.[24] A series of films up to 10 layers thick were studied along with a 135-layer waveguide film. All samples were deposited on glass substrates. In the calculation of the second-order nonlinear optical coefficient, d_{33}, the refractive index of 2.37 (determined by spectroscopic ellipsometry) was used as the index at the harmonic frequency, and a dispersion of 0.05 or less between the harmonic and the fundamental was used. The refractive index was also measured with an equilateral prism-coupling technique in the TM polarization for the 135-layer film; the two numbers were consistent.

Waveguide. The method used to determine waveguide loss was described in a previous study.[25] In the waveguide loss experiment, an argon-pumped Ti:sapphire laser tuned to 800 nm was end-fire coupled into a waveguide, a 135-layer Cop11 film on a glass substrate. When the lowest order mode was excited, a streak was observed in the film. The streak was recorded by a Cortex frame grabber and digitized for data analysis. Another image was digitized with the laser beam blocked to determine the background. Two assumptions were made in the calculation of waveguide loss: the amount of light scattered out of the waveguide was proportional to the amount of light in the waveguide, and the scattering sites were uniformly distributed. The scattered light image was integrated transverse to the propagation direction, and the integrated logarithm of intensity was plotted against the propagation distance. The resulting data were fit (least squares) to a line whose slope is proportional to the loss in dB/cm.

3. Results and Discussion

3.1. Spectroscopic Ellipsometry. Briefly, a spectroscopic ellipsometry measurement determines the change in polarization of a beam of light upon reflection from a surface. The reflectivity of the two polarization components (the s-wave component perpendicular to the plane of incidence and the p-wave component parallel to the plane of incidence) is related to the complex refractive index and the film thickness via the Fresnel equations. It is the relative magnitudes and phases of these two polarization components that give the overall polarization of the light beam. The ellipsometer measures the complex ratio of the reflection coefficients of these two components, in terms of the measured angles Ψ and Δ, where tan (Ψ) is the ratio of the magnitudes of the p- and s-wave reflection coefficients and Δ is the phase difference between the two waves. The standard reference on ellipsometry is the monograph by Azzam and Bashara.[26]

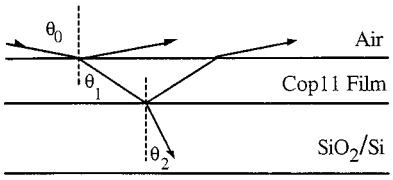

Figure 4. Schematic diagram of a three-layer model showing parallel planes separating air, the multilayers, and the substrate. θ_0 is the angle of incidence, and θ_1 and θ_2 are the angles of refraction that are related by Snell's law.

Analysis of a spectroscopic ellipsometry measurement requires extensive modeling to obtain the refractive index, *n*, the extinction coefficient, *k*, and the film thickness, *h*, of the LB film, since these parameters cannot be directly obtained from the measured angles Ψ and Δ. The optical model used in this analysis is the multilayer structure of air/LB film/SiO_2 film/Si shown in Figure 4. Ψ_{cal} and Δ_{cal} are calculated for the multilayer model using known optical parameters for the substrate, SiO_2 film, and ambient vapor and allowing *n*, *k*, and *h* for the LB film to vary. Ψ_{cal} and Δ_{cal} are then fit to the experimental values of Ψ and Δ using a regression analysis to minimize the mean-square error.[27] Measurements at multiple angles assure an overdetermined system and reliable evaluation of *n*, *k*, and *h*. The LB film was treated as a homogeneous layer. Indeed, further subdivision of the LB film into deposited layers was not possible even with the highest quality data we obtained. The refractive index match between LB layers is within experimental error, especially beyond the first few layers. The reference samples of substrate dipped through the pure air/water interface demonstrated that the SiO_2 layer on the Si wafers could be modeled adequately using the known optical properties of SiO_2.

A complication was that the silicon wafers were made hydrophobic by exposure to hexamethyldisiloxane vapor; the substrate surface contained CH_3 groups. Nevertheless, results of measurements on the treated silicon wafers without LB films showed that we could assume that the thickness of the methylated SiO_2 surface was 20.3 Å and the effective refractive index was that of SiO_2. Explicitly, the data-processing algorithm assumed that at each incident angle and wavelength the optical properties of the substrate remained that of the methylated SiO_2 and that its *n* and *k* variation was that of SiO_2.

From the three 1-layer films (Figure 5), the refractive indices are almost identical. Similar results are obtained for 2-layer and 3-layer films. The numbers obtained from replication were consistent. The optical constants for five different film thicknesses are shown in Figure 6. The refractive index increases approximately ~0.3% with the number of monolayers in the visible region of wavelengths, except those in the region of 650−740 nm. The average refractive index is 2.24 ± 0.15 for these ultrathin films, in which the thickness is small compared to the wavelengths of light. In addition, the refractive index of the 135-layer film, measured with an equilateral prism-coupling technique at a wavelength of 632.8 nm in TM polarization, is 2.37, which implies that the multilayer *n* is equivalent to the bulk value. At wavelengths below 380 nm a slight decrease in the value of the refractive index is observed with the number of layers. Overall, the extinction coefficient is less than 0.5 for wavelengths below the visible range and 0.05 for wavelengths in the visible range.

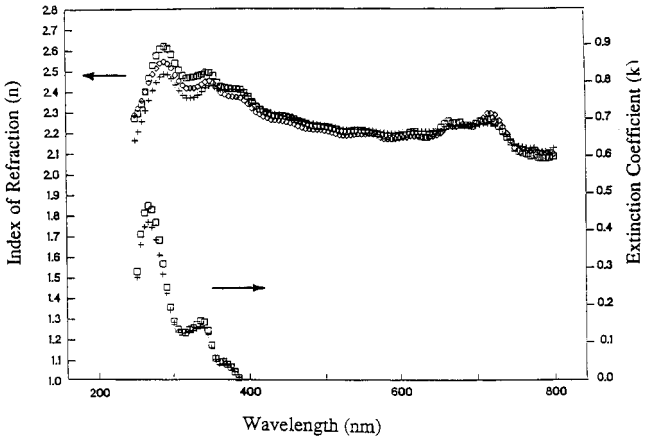

Figure 5. Spectroscopic ellipsometry results for optical constants as a function of wavelength from three angles of incidence, 65, 70, and 75°, for the three samples of a Cop11 monolayer. The index of refraction spectra are nearly coincident in the visible range of wavelengths and are an indication of reproducibility.

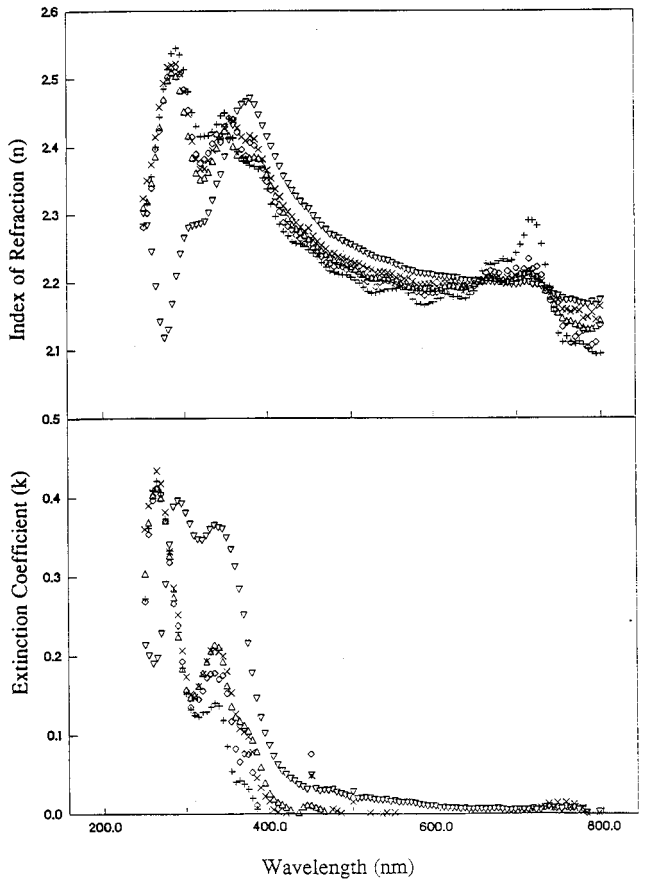

Figure 6. Optical constants as a function of wavelength from three angles of incidence: 65, 70, and 75° for Cop11 films. Five different layer patterns were used: (+) one, (◇) two, (△) three, (×) four, and (▽) ten layers.

The refractive index reported is internally consistent; similar values were obtained for several samples with the same number of layers. In a comparison to other polymeric materials such as bulk poly(pentabromophenyl methacrylate), $n \sim 1.71$,[28] and multilayers of cadmium stearate, $n \sim 1.57$,[29] the Cop11 has a larger value. The chemical makeup of the molecules and close packing in the multilayers are factors contributing to a high index of refraction. Future experiments include measuring the dispersion and birefringence of a bulk sample using the equilateral prism coupling techniques.

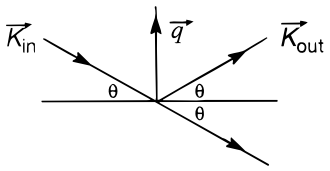

Figure 7. Schematic diagram of the reflectivity experiment. The incident beam strikes the sample surface at an angle θ, and the reflected intensity is recorded by the detector positioning at an angle 2θ. The component of the scattering vector perpendicular to the monolayer is q_z.

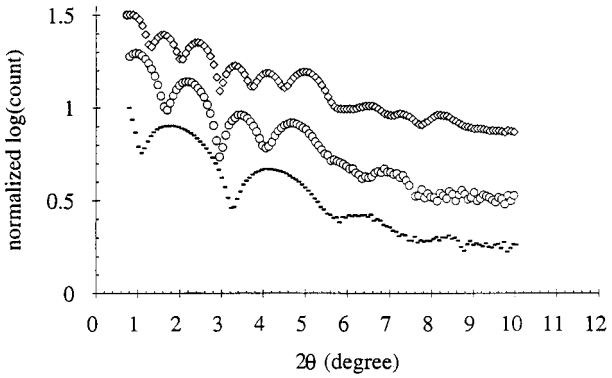

Figure 8. Normalized intensity of reflected X-ray I/I_0, as a function of 2θ for three different thicknesses of Cop11 film: (−) one, (○) two, and (◇) three-layer. The curves (○) and (◇) are offset by 0.25 and 0.5 with respect to curve (−) for clarity. The X-ray reflectivity profiles show that the number of Kiessig fringe peaks corresponds to the number of layers, indicating uniformity in layer thickness.

3.2. X-ray Reflectivity. Synchrotron X-ray reflectivity was also used to determine thickness and structure. X-ray reflectivity measures the intensity, $R(q)$, of the specular reflected X-ray as a function of the angle of incidence. The geometry of the experimental setup, Figure 7, shows that the scattering wavevector is parallel to the z-axis. Thus, the experiment provides a measure of the average variation of the electron density gradient normal to the sample surface. Equation 1 shows that the major contribution to the reflectivity occurs where the expectation value of the gradient, $\langle \cdots \rangle$, is large.

$$R(q) = R_F|\rho_\infty|^{-1} \int_{-\infty}^{+\infty} \langle d\rho_{el}/dz \rangle \exp(iq_z z)\, dz|^2 \qquad (1)$$

where $q_z = 4\pi\lambda^{-1} \sin(\theta)$, R_F is the Fresnel reflectivity, and ρ_∞ is the electron density of the substrate.[30] In multilayers on a substrate the gradients are due to the periodic modulation of electron density in the film and the abrupt change of electron density at the interfaces. As a result, the R vs q_z plot shows Bragg peaks and Kiessig fringes. The analysis of the profile gives information regarding film thickness, electron density, and surface roughness.[31] Kiessig fringes reveal the total film thickness.[32] When the surface roughness increases due to pinholes or stress relaxation, the amplitude of the Kiessig fringes is damped. However, the Bragg peaks are not affected when the roughness is in a micron size scale or larger than the crystallite size.

Figure 8 presents the X-ray reflectivity data for the 1, 2, and 3-layer samples. Increasing thickness yields closer fringe spacings. For a given 2θ range (e.g., 1−2.5°) the number of maxima corresponds to the numbers of monolayers. Figure 9 shows the X-ray reflectivity profile for the 10-layer Cop11 sample with the Kiessig fringes. We calculate that the average

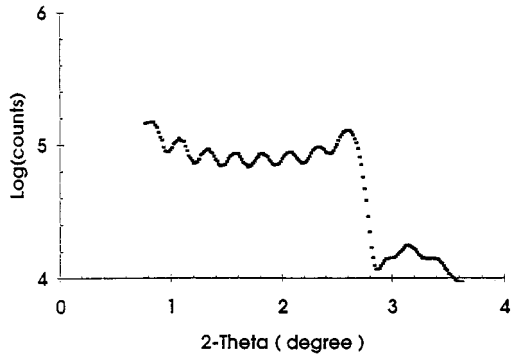

Figure 9. Reflected X-ray intensity as a function of 2θ for a ten-layer Cop11 film. In addition to showing Kiessig fringes, the reflectivity profile exhibits a Bragg peak at $2\theta = 2.6°$.

Table 1. Estimated Film Thickness of Cop11[a]

no. of layers	ellipsometry (Å)	X-ray reflectivity	X-ray diffraction
1	39.7	39.27	
2	74.0 (37)	73.90 (36.95)	
3	116.8 (38.9)	114.3 (38.1)	
10	394 (39.4)	359.3 (35.93)	(35)

[a] In parentheses are average values of thickness per layer, $\langle \Delta h \rangle$.

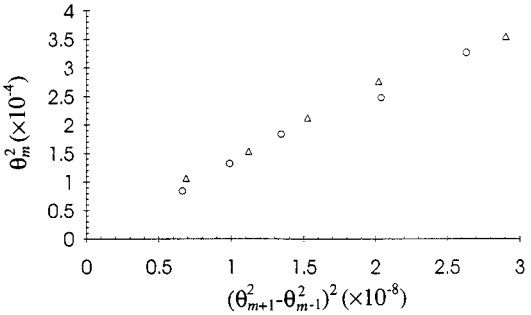

Figure 10. Plot of θ^2_m versus $(\theta^2_{m+1} - \theta^2_{m-1})^2$. From angular positions of the maxima (○) and the minima (Δ) of Kiessig fringes for a ten-layer Cop11 film. Linear regression gives an intercept of 0.09×10^{-4} radian and a slope of 1.19×10^4.

monolayer thickness is larger than the X-ray diffraction value of 35.0 Å, Table 1. In addition, the 10-layer sample shows a Bragg peak, suggesting an ordered film formation. A rough estimation of the structural parameters is obtained using the Koenig and Carron equation[33,34]

$$\theta^2_m = (\theta^2_{m+1} - \theta^2_{m-1})^2 h^2/4\lambda^2 + \theta^2_c \qquad (2)$$

where h is the total film thickness and m is the order of the interference fringe. θ_m is the reflection angle of the mth fringe, and θ_c is the critical angle for total external reflection. Plotting $(\theta^2_{m+1} - \theta^2_{m-1})^2$ versus θ^2_m yields θ^2_c from the y-intercept and h from the slope, Figure 10. Each layer thickness, Δh_m, is estimated with the Wainfan and Parratt equation.[35]

$$\Delta h_m = \lambda/4(\theta^2_m - \theta^2_c)^{1/2} \qquad (3)$$

From Figure 10 the analysis of the 10-layer film gave h = 355.2 Å and θ_c = 0.172°. This gives an electron density of 0.378 Å^{-3} and the mass density of 1.16 g/cm^3 (assuming the monolayer consists of alternating monomer units attached to a siloxane backbone). Using the values of the electron density, the total number of electrons in the two monomers (432), and the average

monolayer thickness, the projected area of the repeat unit is calculated, giving a value of 31 ± 2 Å^2. This is close to the coarea of a close-packed monolayer, 27 Å^2, at the air−water interface. The surface roughness was calculated to be ∼2.8 Å. The accuracy in the measurement of thickness has an uncertainty of less than 8%, compared to the fully extended chain obtained from X-ray diffraction. In Table 1, a different procedure is used to find the film thickness by taking the 2θ separation of two consecutive peaks and applying the relation $\Delta h = 0.5\lambda/\Delta(\sin\theta)$. All values are in Angstroms and those in parentheses are the average values.

The estimated film thickness of Cop11 as measured by ellipsometry and X-ray reflectivity is summarized in Table 1. The result from X-ray diffraction is the same as obtained from a previous study.[22] For the 10-layer film, the average monolayer thickness from the two X-ray methods is nearly equal. However, from X-ray reflectivity, thicker samples have a smaller average monolayer thickness. The multilayer film thicknesses are comparable to those measured by ellipsometry. In the X-ray reflectivity measurement, the film thickness is the distance separating the interfaces of media of different electron densities. The electron density or index of refraction of $Si(CH_3)_3$, which is used to "attach" the monolayers to the substrate, is nearly the same as SiO_2.[36,37] Hence, with chemisorbed $Si(CH_3)_3$ the X-ray analysis includes the methyl groups as a part of the monolayer. This marks a difference between the monolayer film thickness and the average thickness of the multilayer film of ∼1 Å.[27] For a thick film the contribution of the $Si(CH_3)_3$ is minimal. For the 10-layer sample the slightly different value measured by the ellipsometry could be attributed to experimental uncertainty of the model used in the data reduction. Overall, these results suggest that the side chains of the copolymer are oriented normal to the substrate.

3.3. Monolayer Formation of Cop11,4. The pressure−area isotherm for the monomer of Cop11,4 is shown in Figure 2. The isotherm indicates that a kink occurred at 8 mN/m and could be a collapse pressure. The extrapolation to zero surface pressure gave a coarea of 28 Å^2/repeat unit. The behavior of the polymer at the interface can be described using a scaling law argument.[38] The osmotic compressibility can be expressed in terms of the scaling exponent as a function of polymer concentration in a semidilute concentration region. An equivalent expression is given as[39]

$$\pi \sim A^{-y} \tag{5}$$

where $y = 2\nu/(2\nu - 1)$. π is the surface pressure of the polymer, A is the area occupied per repeat unit at the interface, and ν is the characteristic scaling exponent. In a dilute polymer concentration, ν relates the dependence of the radius of gyration to the polymer's molecular number for a given solvent. For a good solvent ν is 0.77 and for a poor solvent ν is 0.51.[40] Here, the air−water interface is taken as the solvent. Figure 11 is a log−log plot of the π−area isotherm of Cop11,4. There are three linear segments, and a scaling parameter ν can be estimated for each. The experimental data between the surface pressure of 0.71 and 6.1 mN/m (the middle segment in Figure 10) give $\nu = 0.52$. The low-pressure segment gives $\nu = 0.61$. The high-pressure segment gives $\nu = 1.5$. The scaling exponent of $\nu = 0.52$ implies that the copolymer at the air−water interface behaves as though it is in a Θ solvent. When first dropwise spread from a solvent, the copolymer molecules might aggregate but as the solvent evaporates, they occupy a relatively large area per repeat unit. In this state $\nu = 0.61$, which suggests that the interface is behaving as a good solvent. Presumably, at the kink at about 28 A^2/repeat unit, islands of extended molecules contact each other and then folded horizontally. (Further experiments are needed to confirm this, e.g., Brewster angle microscopy.) It is likely that collapse sets in at about 25 A^2/repeat unit. The high-pressure segment gave $\nu = 1.5$. It is clear that three-dimensional structures are being formed in the high-pressure segment of the isotherm. This behavior was confirmed by creep experiments shown in Figure 3. In comparison to $\nu = 0.52$, the scaling exponent of Cop11 is 0.58, exhibiting a behavior similar to that of Cop11,4. A possible explanation of the behavior of the copolymer at the air−water interface is that at low pressure some parts of the coiled siloxane main chain are anchored to the water surface through the oxygen atoms.[41,42] With increasing surface pressure, the main chain is compressed into a tightly coiled configuration[43] and exposes the hydrophilic methoxy−ethoxy−methoxy (MEM) groups of the side-chains. Thus, the side chains point toward the water and can get close to each other to be close-packed perpendicular to the plane of the monolayer. In contrast, for Cop11,4 the lack of MEM groups causes the copolymer to attach poorly at the air−water interface.

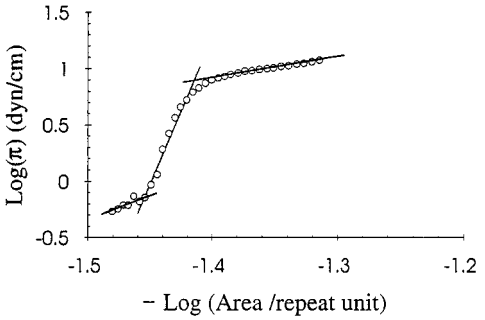

Figure 11. log−log plot of surface−pressure (π) versus area per repeat unit for the Cop11,4 monolayer along with the fit to eq 5 done in three segments.

Cop11,4 was poorly dissolved in chloroform. The monolayer shows holes and impingement lines of islands. When the film was spread in methylene chloride, the quality of the monolayer was improved; there were fewer holes. The film was highly rigid. Deposited on the substrate, the film gave an opaque appearance. In Figure 3, the compressive creep curve shows a 3% area change at 5.4 mN/m. At longer compression times, the film was less stable when the pressure on it was increased from 5.4 to 9.5 mN/m. The creep results at 17.4 mN/m suggest the monolayer collapsed completely, as indicated by a continuous dropping of surface pressure with time.

3.4. Waveguide Loss. The results from the waveguide experiment give an indication of the film quality. A photograph of light propagating in a guide is shown in Figure 12. The important parameters in waveguide propagation are the film thickness, the refractive index of all media, and the optical loss.[44] The thickness of the 135-layer Cop11 film is approximately 0.47 μm. The length of the light streak in Figure 12 is ∼2 cm (Table 2). Waveguide losses in the range of 1.7−5.0 dB/cm were observed for TE modes (not uniform over the surface or between samples). These losses are similar to those observed in other LB films[3,10] We have

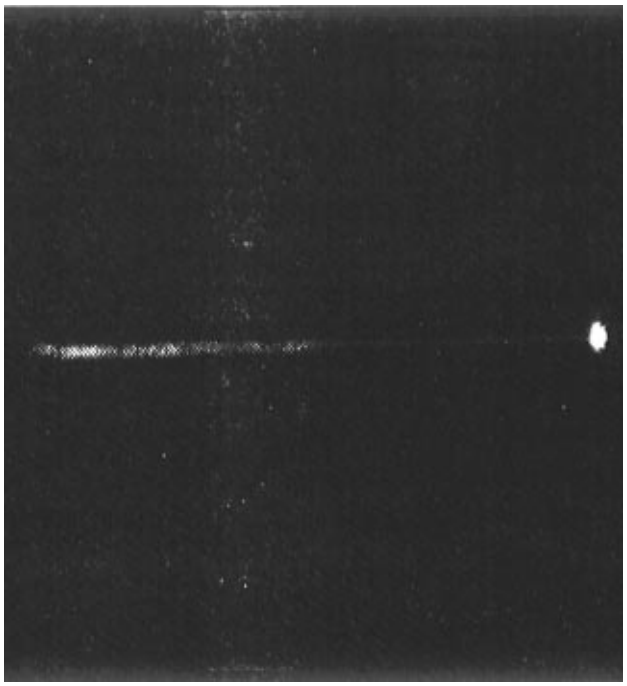

Figure 12. Photograph of the light streak in a 135-layer Cop11 film at a wavelength of 800 nm in transverse electric polarization. Light is coupled into the film at the left-hand side and comes out from the edge of a glass slide. The defect sites are apparently nonuniformly distributed.

Table 2. Cop11 Optical Measurements

waveguide		SHF	
thickness	135 layers	d_{33}	42.0 ± 1.7 pm/V
mode	TE	d_{33}/d_{31}	40.1
wavelength	800 nm		
loss	2.3 ± 0.5 dB/cm		

calculated the optical intensity profile for the guided mode using the measured optical constants and thickness. It indicates that 97% of the optical energy is located within the waveguide, as would be expected from such high refractive index films. This means that the measured waveguide loss well represents the intrinsic loss in the waveguide. Due to the nonuniformity of the loss, it likely arises predominantly from scattering loss. The low losses reported here are likely due to the copolymeric nature of the films, which limits crystallite size and may serve to inhibit highly misaligned microcrystallite formation in the films. The highly polar structure perpendicular to the film plane may also inhibit large index of refraction fluctuations in the plane of the film. Controlling the fabrication step of LB films can reduce the scattering. Figure 6 indicates very low absorption loss at 800 nm. However, it is seen that absorption increases in the visible region, and may become the limiting factor for waveguide loss.

3.5. Second Harmonic Generation. The results for second harmonic generation are shown in Figure 13. The figure indicates that the highly aligned structure observed in films up to 10 monolayers thick is maintained at a level of about 70% up to the thickness of the 135 layer films. Thus, even the thick films are indeed highly polar. The measured value of second harmonic coefficient is $d_{33} = 42.0 \pm 8.0$ pm/V. This value is nonresonant since the first absorption band is below 400 nm and is considerably larger than previously reported.[15] In our earlier publication, the index of refraction had not been measured and an index of refraction of approximately 1.5 was assumed. The large

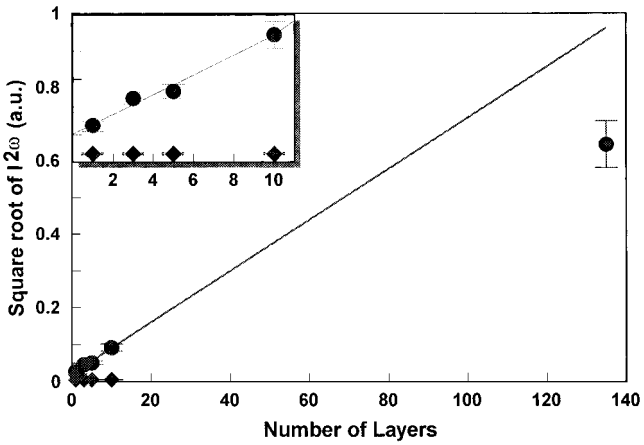

Figure 13. Square root of the second harmonic generation intensity (proportional to the susceptibility) for Cop11 films as a function of the number of layers. Results for p (circles) and s (diamonds) incident polarizations with the *p* polarized second harmonic indicating the large anisotropy are shown. The inset is the magnified lower left corner of the larger figure.

refractive indices reported here indicate that our nonlinear optical coefficient was significantly underestimated previously. Since the measured nonlinear coefficient is about 70% of that expected from the extrapolation from much thinner films, one would conclude that the orientation is not as polar as reported in the thinner films.

We can roughly estimate the molecular response in terms of the measured film susceptibility. The relationship between the molecular and film susceptibility for d_{33} where the 3 direction is perpendicular to the film is given by[12,15]

$$d_{33} = N f^{\omega} f^{\omega} f^{2\omega} \beta_{zzz} \langle \cos^3 \theta \rangle \qquad (6)$$

where N is the number density of molecules in the film, f's are local field factors given by $f^{\omega} = (n_{\omega}^2 + 2)/3$, and θ is the angle between the molecular z-axis (dipole axis) and the film 3 axis. The average value of this angle was determined previously to be approximately zero.[15] Here we will assume that $\langle \cos \theta \rangle \approx 0.7$ from Figure 13. The number density can be calculated from the inverse molecular volume as determined from the monolayer isotherm and the layer spacing. This is $N = 1/(25\ \text{Å}^2 \times 35\ \text{Å}^2) \approx 1 \times 10^{21}/\text{cm}^3$. The local fields are calculated from $n = 2.37$. Thus we calculate B $\approx 9 \times 10^{-30}$ esu, which is in good agreement with previously measured values.[15] Note that the reported error bars above include the fact that birefringence was ignored in the data analysis. This large second harmonic coefficient is nonresonant at a 1.06 mm pump, as indicated by the extinction coefficient seen in Figure 6.

An attempt to double the d_{33} by replacing the Cop11's MEM groups with NO_2 groups resulted in the synthesis of Cop11,4. However, Cop11,4, which has spacer lengths of eleven and four carbon atoms, formed an unstable monolayer because the shorter spacer length broke the packing too much and could not reduce the hydrophobicity to compensate for the loss of the MEM groups, which served to enhance the spreading. A study by Jarvis[43] shows that the homopolymer of poly(methyl(x-alkyl)siloxanes) failed to spread as a monolayer film when the alkyl group contained more than $x = 8$ carbon atoms. Thus, a proper choice of the polarity of the mesogenic group can help the molecules spread even though a long spacer length is used.

4. Conclusion

The index of refraction of Cop11 is relatively high compared to those of other optical polymeric materials. Though low optical losses were measured at 800 nm, absorption may be problematic at shorter wavelengths, indicating that Cerenkov phase-matching may be favored. The film thicknesses measured by ellipsometry and X-ray reflectivity support the previous study, suggesting that the side chains of the copolymer are oriented perpendicular to the substrate surface. For thick LB films, pinhole and layer defects cause light scattering that attenuates light transmission. The measured optical nonlinearity is very large and is due to the high density and degree of polar order in the films. The measured second harmonic coefficient is consistent with an oriented gas model for the molecules. The second-order nonlinear susceptibility can be increased by increasing the surface density of the NLO group. Although Cop11,4 has twice the NLO groups relative to Cop11, poorly oriented structure results in a nondetectable second harmonic signal. For Cop11, the high nonlinear optical susceptibility combined with its ability to be formed into multilayer film makes it an excellent candidate material for nonlinear optical integrated devices.

5. Acknowledgment

The support of this work by the Advanced Liquid Crystal Optical Materials program under NSF grant No. DMR-8920147 is gratefully acknowledged. The ellipsometry experiments were performed at Sandia National Laboratories, which is supported by the Department of Energy under contract number AC04-94AL85000.

References and Notes

(1) Ulman, U. *An Introduction to Ultrathin Organic Films;* Academic Press: Boston, 1991; Chapter 2.
(2) Motschmann, H. R.; Penner, T. L.; Armstrong, N. J.; Ezenyilimba, M. C. *J. Phys. Chem.* **1993**, *97*, 3933.
(3) Clays, K.; Armstrong, N. J.; Ezenyilimba, M. C.; Penner, T. L. *Chem. Mater.* **1993**, *5*, 1032.
(4) Clays, K.; Armstrong, N. J.; Penner, T. L. *J. Opt. Soc. Am. B* **1993**, *10*, 886.
(5) Penner, T. L.; Motschmann, H. R.; Armstrong, N. J.; Ezenyilimba, M. C.; Williams, D. J. *Nature* **1994**, *367*, 49.
(6) Wijekoon, W. M. K. P.; Wijaya, S. K.; Bhawalkar, J. D.; Prasad, P. N.; Penner, T. L.; Armstrong, N. J.; Ezenyilimba, M. C.; Williams, D. J. *J. Am. Chem. Soc.* **1996**, *118*, 4480.
(7) Bosshard, Ch.; Kupfer, M.; Florsheimer, M.; Gunter, P. *Thin Solid Films* **1992**, *210*, 153.
(8) Kupfer, M.; Florsheimer, M.; Bosshard, Ch.; Gunter, P. *Electron. Lett.* **1993**, *29*, 2033.
(9) Kupfer, M.; Florsheimer, M.; Baumann, W.; Bosshard, Ch.; Gunter, P.; Tang, Q.; Zahir, S. *Thin Solid Films* **1993**, *226*, 270.
(10) Bosshard, Ch.; Otomo, A.; Stegeman, G. I.; Kupfer, M.; Florsheimer, M.; Gunter, P. *Appl. Phys. Lett.* **1994**, *64*, 2076.
(11) Ou, S. H. Ph.D. Dissertation, Case Western Reserve University, Cleveland, OH, 1992, Chapter 3.
(12) Shen, Y. R. *Nature* **1989**, *337*, 519.
(13) Singer, K. D.; Sohn, J. E.; King, L. A.; Gordon, H. M.; Katz, H.; Dirk, C. W. *J. Opt. Soc. Am.* **1989**, *B6*, 1339.
(14) Shi, S. *Contemporary Phys.* **1994**, *35*, 2.
(15) Ou, S. H.; Percec, V.; Mann, J. A.; Lando, J. B.; Zhou, L.; Singer, K. D. *Macromolecules* **1993**, *26*, 7263. Ou, S. H.; Mann, J. A.; Lando, J. B.; Zhou, L.; Singer, K. D. *Appl. Phys. Lett.* **1992**, *61*, 2284.
(16) Percec, V.; Ungar, G.; Heck, J. *Macromolecules* **1991**, *24*, 4957.
(17) Hallensleben, M. L.; Kabus-Henke, A. *Polym. Bull.* **1992**, *28*, 251.
(18) Bautista, O. M.; Duran, R. S.; Ford, W. T. *Macromolecules* **1993**, *26*, 659.
(19) Munn, R. W.; Ironside, C. N. *Principles and Application of Non-linear Optical Material*; Blackie Academic & Professional: New York, 1993; Chapter 9.
(20) Gaines, G. L. *Insoluble Monolayers at liquid Gas Interface*; Interscience Publishers: New York, 1966; Chapter 4.
(21) Robert, G. G.; Petty, M. C.; Baker, S.; Fowler, M. T.; Thomas, N. J. *Thin Solid Films* **1985**, *132*, 113.
(22) Jansson, R.; Arwin, H.; Gustafsson, G.; Inganas, O. *Synth. Met.* **1989**, *28*, C371.
(23) Prasad, P. N.; David, D. J. *Introduction to Nonlinear Optical Effect in Molecules and Polymer*; John Wiley: New York, 1991; p 177.
(24) Kuzyk, M. G.; Singer, K. D.; Zahn, H, E.; King, L. A. *J. Opt. Soc. Am.* **1989**, *B6*, 742.
(25) Hubbard, S. F.; Singer K. D.; Li, F.; Cheng, S. Z. D.; Harris, F. W. *Appl. Phys. Lett.* **1994**, *65*, 265.
(26) Azzam, R. M. A.; Bashara, N. M. *Ellipsometry and Polarized Light*; North-Holland: Amsterdam, 1997.
(27) Alterovitz, S. A.; Bu-Abbud, G. H.; Woolam, J. A.; Liu, D. C. *J. Appl. Phys.* **1983**, *54*, 1559.
(28) *Polymer Handbook*; Brandrup, J., Immergut, E. H., Eds.; John Wiley: New York, 1975; VI-451-VI-461.
(29) Pitt, C. W.; Walpita, L. M. *Thin Solid Films* **1980**, *68*, 101.
(30) Wasserman, S. R.; Whiteside, G. M.; Tidwell, I. M.; Ocko, B. M.; Pershan, P. S.; Axe, J. D. *J. Am. Chem. Soc.* **1989**, *111*, 5852.
(31) Rieutord, F.; Benattar, J. J.; Rivoira, R.; Lepetre, Y.; Blot, C.; Luzet, D. *Acta. Crystallogr.* **1989**, *A45*, 445.
(32) Mensinger, H.; Stamm, M.; Boeffel, C. *J. Chem. Phys.* **1992**, *96*, 3183.
(33) Roberts, K. J.; Sherwood, J. N.; Shripathi, T.; Oldman, R. J.; Holmes, P. A.; Nevin, A. *J. Phys. D: Appl. Phys.* **1990**, *23*, 255.
(34) Koenig, J. H.; Carron, G. J. *Mater. Res. Bull.* **1967**, *2*, 509.
(35) Wainfan, N.; Parratt, L. G. *J. Appl. Phys.* **1960**, *31*, 1331.
(36) Konovalov, O. V.; Feigin, L. A. *J. Phys. IV* **1993**, *3*, 185.
(37) Geer, R. E.; Chen, M. S.; Calvert, J. M.; Shashidhar, R.; Jeong, Y. H.; Pershan, P. S. *Langmuir* **1994**, *10*, 1171.
(38) de Gennes, P. G. *Scaling Concepts in Polymer Physics*; Cornell University Press: Ithaca, NY, 1979.
(39) Zhu, Y. M.; Lu, Z. H.; Wei, Y. *Phys. Rev. E* **1994**, *49*, 5316.
(40) Adam, J.; Buske, A.; Duran, R. S. *Macromolecules* **1993**, *26*, 2871.
(41) Kalacher, A. A.; Litvinov, V. M.; Wegner, G. *Makoromol. Chem. Macromol. Symp.* **1991**, *46*, 365.
(42) Noll, W.; Steinbach, H.; Sucker, C. *J. Polym. Sci., Part C* **1971**, *34*, 123.
(43) Jarvis, N. L. *J. Polym. Sci., Part C* **1971**, *34*, 101.
(44) Burzynski, R. *Appl. Phys. Lett.* **1988**, *53*, 2011.

MA961256L